



1 **Research on clock synchronization method of marine**
2 **controlled source electromagnetic transmitter base on**
3 **coaxial cable**

4 Zhibin Ren¹, Meng Wang¹, Kai Chen¹, Chentao Wang¹, Runfeng Yu¹

5 ¹China University of Geosciences (Beijing), School of Geophysics and Information Technology, Beijing
6 CO 100083, China

7 *Correspondence to:* Meng Wang (wangmeng@cugb.edu.cn).

8 **Abstract.** Marine controlled source electromagnetic (MCSEM) method is widely used to reveal the
9 electrical structure of shallow media below the seafloor. It is an indispensable geophysical means in the
10 exploration of marine oil and gas exploration, natural gas hydrates and seafloor geological structures.
11 The transmitter and receiver in electromagnetic detection equipment need to maintain a high temporal
12 consistency, usually using high-stability pulse-per-second (PPS) generated by GPS or BeiDou navigation
13 modules as a synchronization signal. Coaxial cable is a widely used tow cable, so it is necessary to design
14 a clock synchronization method of marine controlled source electromagnetic transmitter using coaxial
15 cable. This paper proposes a method for synchronizing the internal clocks of the transmitter with PPS
16 using ship-borne power supply when coaxial cable is used as tow cable. In this method, the ship-borne
17 high-power supply outputs a high-voltage AC signal that is synchronized with the 400 Hz signal output
18 from GPS; the coaxial cable transmits AC high-power electrical energy and control commands; the AC
19 signal transmitted via the coaxial cable is converted into a stable and continuous 1 Hz signal by step-
20 down, waveform shaping and frequency division for synchronizing the internal time pulses of the
21 transmitter. The test result shows that the 1 Hz signal obtained by this method has a deviation of about
22 504 ns relative to the PPS. This deviation meets the need of MCSEM transmitter for clock
23 synchronization.

24 **Keywords:** marine controlled source electromagnetic, coaxial cable, transmitter, clock synchronization

25
26 **1 Introduction**

27 Marine controlled source electromagnetic (MCSEM) method is one of the methods in exploration of
28 seafloor natural gas hydrates (Edwards and Chave, 1986; Cox et al., 1986). It is an indispensable
29 geophysical means in the exploration of marine oil and gas exploration, natural gas hydrates and seafloor
30 geological structures (Constable and Srnka, 2007; Constable, 2010). In MCSEM method, the
31 synchronization of the internal clocks of the transmitter and receiver is a very important issue (Wang et
32 al., 2015; Meng et al., 2009). Electromagnetic data processing and interpretation depend on the
33 synchronization between the transmitter and receiver (Qiu et al., 2020). The MCSEM transmitter and
34 receiver are separated from each other (Chen et al., 2012; Chen et al., 2020), and they are not connected
35 by any cable. Therefore, Pulse-Per-Second (PPS) signal output from GPS is used as a common
36 synchronization signal to synchronize the internal clock of transmitter and receiver.

37 The commonly used tow cables for MCSEM transmission systems are photoelectric composite cables
38 and coaxial cables. The transmitter's clock synchronization method varies based on the type of tow cable.
39 When using coaxial cable as a tow cable, clock synchronization can be achieved by controlling power
40 supply output or transmitting PPS to the transmitter before it is submerged. As an example, SUESI-500
41 transmitter of Scripps Institution of Oceanography uses a standard UNOLS 0.680 inch (17.27 mm)



42 coaxial cable as tow cable. They use a 400 Hz output from a GPS clock to generate a 400 Hz sine wave
43 of variable amplitude to control the power supply (Constable, 2013; Constable, 2006). SUESI-500
44 transmitter's frequency control signals is generated based on 400 Hz signal. GPS time provided by the
45 power signal is used to clock the time-related functions. When using photoelectric composite cable as a
46 tow cable, clock synchronization can be achieved by transmitting PPS through one channel of the
47 optical fiber. For example, the transmitter of China University of Geosciences (Beijing) uses a 32.8 mm
48 photoelectric composite cable as the tow cable, and its clock synchronization is achieved by transmitting
49 PPS and GPS time through the optical fiber (Wang et al., 2021). However, the cost of photoelectric
50 composite cable is high and generally only large scientific research ships can be equipped. In order to
51 enable MCSEM transmitters work on more ships, using coaxial cable is necessary. However, coaxial
52 cable has only one message channel compared to photoelectric composite cable and can't be assigned a
53 separate channel to transmit PPS. The coaxial cable uses power line communication to transmit data and
54 commands, but signal delay is unstable. If PPS is transmitted via coaxial cable, it will have a large
55 deviation. Consequently, how to use coaxial cable to synchronize internal clock of MCSEM transmitter
56 is a challenging problem. This paper proposes a clock synchronization method of MCSEM transmitter
57 based on coaxial cable. In this method, the sinusoidal signal from the power supply is synchronized with
58 the 400 Hz square wave signal from GPS; The sinusoidal power signal transmitted to the underwater
59 transmitter is converted into a stable and continuous 1 Hz square wave signal by step-down, waveform
60 shaping and frequency division. The 1 Hz square wave signal is as the synchronization signal for the
61 transmitter's internal clock.

62 2 Clock synchronization based on coaxial cable

63 In this paper, the tow cable used is a coaxial cable. This coaxial cable not only transmits electrical energy
64 but also functions as a communication link between the deck monitoring terminal and underwater
65 transmitter. Communication is achieved through power line communication technology (Ferreira et al.,
66 2001; Amuta et al., 2020), utilizing a differential chaos shift keying coding scheme (Kaddoum and
67 Tadayon, 2016). The power transmitted through the coaxial cable is a 400 Hz sinusoidal waveform. Fig.1
68 illustrates the structure of the coaxial cable, where the innermost layer consists of a conductive copper
69 core surrounded by an insulating medium. The insulating medium is encased by a mesh conductor, which
70 provides electromagnetic shielding. The outermost layer is an insulating protective sheath.

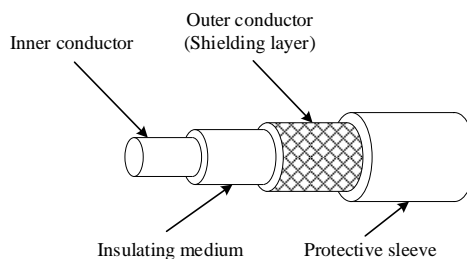


Fig.1 The structure diagram of coaxial cable.

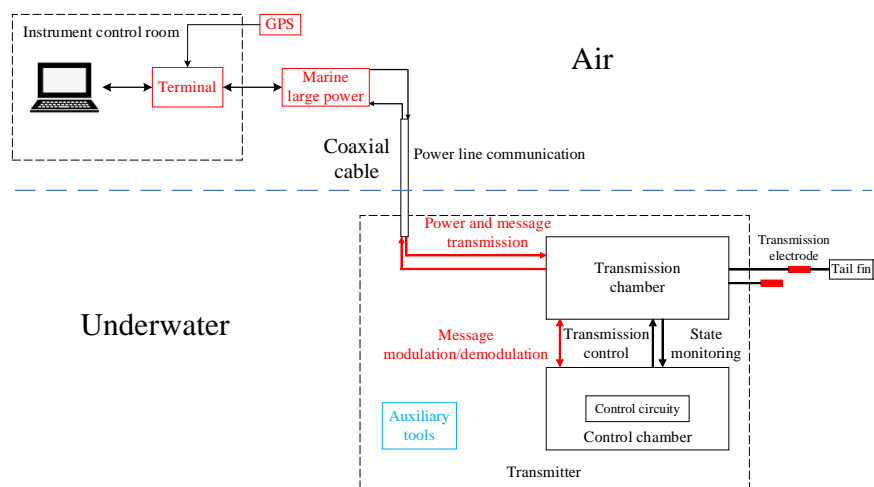
71
72

73

74 Fig.2 illustrates the schematic diagram of the MCSEM transmission system, which is based on a coaxial
75 cable. The ship is equipped with an instrument control room used to house the computer and deck
76 monitoring terminal. The deck monitoring terminal is connected to the ship-borne high-power supply,
77 allowing it to control power on/off functions and facilitating communication with the underwater
78 transmitter. The deck monitoring terminal also receives GPS time messages and PPS for clock



79 synchronization. The ship-borne high-power supply generates 0~3000 V/400 Hz AC electricity to power
 80 the underwater transmitter (Wang et al., 2017b). In addition to transmitting electrical energy, the coaxial
 81 cable also transmits commands to the underwater transmitter via power line communication. The
 82 underwater transmitter consists of two main components: a transmission chamber and a control chamber.
 83 The the transmission chamber houses the step-down, rectification and inverter units, which transmit high
 84 power electromagnetic waves to the seafloor (Meng et al., 2015). The control chamber contains the
 85 control circuit for the entire transmitter, allowing it to transmit frequency-switching signals to control
 86 high-current transmission and monitor the transmitter's state parameters. The transmitter is also equipped
 87 with auxiliary tools such as an altimeter and an attitude module to measure safety-related parameters
 88 during underwater towing. The transmitter electrodes are towed behind the transmitter (Wang et al.,
 89 2013), with a tail fin attached to the electrodes to stabilize their orientation (Wang et al., 2013; Wang et
 90 al., 2017a; Liu et al., 2012).



91
 92 **Fig.2 The schematic diagram of MCSEM transmission system based on coaxial cable.**
 93

94 Fig.3 illustrates the synchronization signal flow based on a coaxial cable. The GPS module features a
 95 TIMEPULSE pin that can be configured to output a 400 Hz square wave, with its rising edges precisely
 96 aligned with the PPS at integer seconds. The deck monitoring terminal contains a signal follower that
 97 receive 400 Hz square wave from the GPS and transmits it to the ship-borne high-power supply. The 400
 98 Hz AC output from the power supply is synchronized with the 400 Hz square wave. To prevent
 99 interference from the high-power supply, the signal between the deck monitoring terminal and the power
 100 supply is transmitted via an isolated RS485 bus. The 400 Hz sinusoidal signal generated by the high-
 101 power supply is transmitted to the underwater transmitter through the coaxial cable, where it is converted
 102 to a sinusoidal signal in the range of 0~22 V by two transformers. The signal processing unit in the
 103 transmitter's control circuit processes the 0~22 V sinusoidal signal and generates a 1 Hz square wave as
 104 the synchronization signal for the control circuit. The rising edges of 1 Hz square wave are aligned with
 105 the rising edges of PPS.

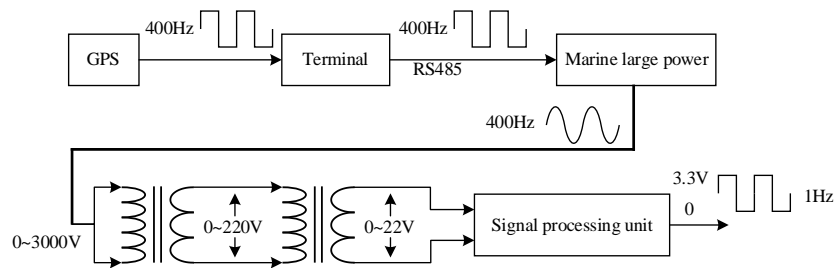


Fig.3 The flow diagram of synchronization signal.

106
 107
 108

3 Hardware design of clock synchronization method based on coaxial cable

3.1 Deck monitoring terminal

109
 110
 111 Fig.4 presents the block diagram of the deck monitoring terminal. The deck monitoring terminal
 112 comprises a communication module and a coaxial cable modulation/demodulation module (modem). The
 113 communication module facilitates interaction between the monitoring software on the PC and the
 114 transmitter. A signal follower within the communication module receives the 400Hz signal output from
 115 the GPS and relays it to the high power power supply as a synchronization signal. The coaxial cable
 116 modem modulates the messages sent by the PC onto the two power lines of the coaxial cable and
 117 demodulates the messages returned by the transmitter through the coaxial cable.

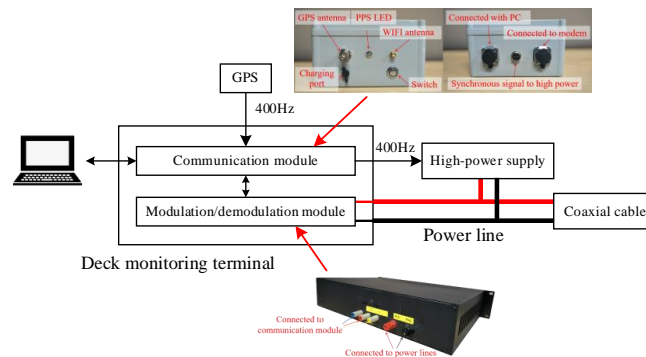


Fig.4 The block diagram of deck monitoring terminal.

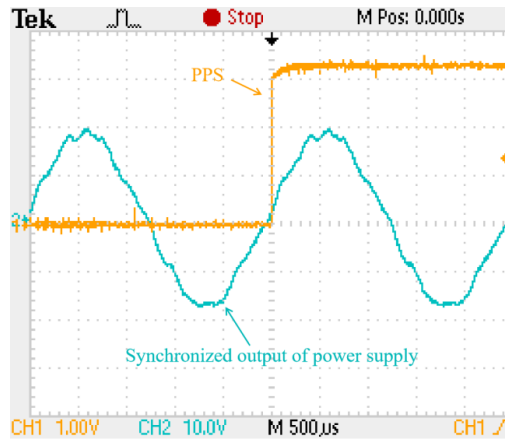
118
 119
 120

3.2 High-power supply output synchronized with GPS

121
 122 The high-power supply is designed with a synchronization signal access function to accept external
 123 synchronization signals. It outputs a synchronized sinusoidal signal aligned with the externally connected
 124 synchronization signal. Both the underwater transformer of transmitter and the ship-borne high-power
 125 supply operate at a frequency of 400 Hz. Accordingly, the TIMEPULSE pin of the GPS is configured to
 126 output a 400 Hz signal and is connected to the high-power supply via the communication module. The
 127 power supply output voltage is set to 20V. Another TIMEPULSE pin on the GPS is configured to output
 128 a 1 Hz signal, which is monitored alongside the power supply output. Fig.5 shows the synchronized
 129 output signal waveform of power supply. It can be observed that the zero phase of the power output
 130 signal is aligned with the rising edge of the PPS. After continuous observation, the 400Hz sinusoidal
 131 signal output from the power supply remains stable relative to the rising edges position of the PPS. This



132 synchronization of the power supply output is effective, and forms the foundation of the entire clock
133 synchronization method.

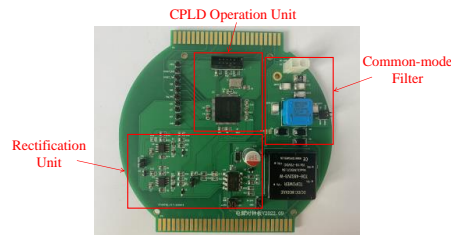
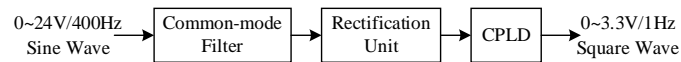


134
135
136

Fig.5 The synchronized output signal waveform of power supply.

137 3.3 Signal processing unit

138 The 400 Hz sinusoidal signal output from the high-power supply is transmitted to the transmitter via a
139 coaxial cable. It passes through two transformers and is converted into a sinusoidal wave with an
140 amplitude ranging from 0 to 24 V. This signal is then converted into 1 Hz square wave with an amplitude
141 of 1 to 3.3 V by the signal processing circuit. Fig.6 shows the hardware of signal processing unit.



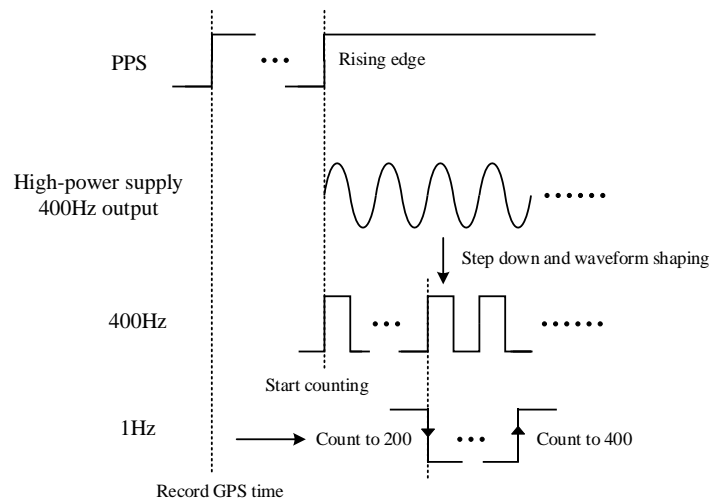
142
143
144

Fig.6 The hardware of signal processing unit.

145 The 400 Hz sinusoidal wave, ranging from 0 to 24 V, is first processed by a common-mode filter to
146 eliminate noise. A protective circuit, consisting of gas discharge tubes (GDT) and transient voltage
147 suppression (TVS) diodes, surrounds the common-mode filter circuit to prevent over-voltage and protect
148 the subsequent stages. After filtering, the sinusoidal wave is processed through a rectification unit, which
149 converts it into a 0~3.3 V, 400 Hz square wave signal. This rectification unit comprises an optical coupler
150 and an operational amplifier, which rectifies the signal, isolates the input from the output, and protects
151 the following operational circuits from sudden variations in the input signal. The square wave signal from
152 the rectifier is then processed by the operation unit of the underwater signal processing system, which
153 generates a 1 Hz square wave using a pulse counting method. The core of the operation unit is a complex
154 programmable logic device (CPLD), which outputs one rising edge for every 400 rising edges of the 400



155 Hz square wave. The 1 Hz square wave output from the CPLD operation unit is the final synchronization
156 signal transmitted to the control circuit.
157 To align the rising edges of the 1 Hz square wave with the rising edges of the PPS, the CPLD module
158 records the exact moment of the PPS rising edges. The 1 Hz square wave is aligned with the PPS only
159 when the CPLD begins counting the 400 Hz square wave at the moment of a PPS rising edge. Therefore,
160 before submerging the transmitter, an external GPS module is connected to it. Once the CPLD records
161 the timing of the PPS rising edges, it generates an internal 1 Hz signal synchronized with the PPS.
162 Afterward, the external GPS module is removed, and the power supply is activated. The CPLD module
163 initially sets the output pin to low and then, raises it high upon detecting the first rising edge of the
164 internally generated 1 Hz signal, as illustrated in Fig.7. After this, when the rising edge count of the 400
165 Hz signal reaches 200, the output pin is set to low, generating a falling edge; when the count of the 400
166 Hz signal reaches 400, the output pin is set to high, generating a rising edge and resetting the counter
167 for the next cycle. The clock synchronization of the entire transmitter system depends on the rising edges
168 of the PPS, which must be generated with accuracy and stability. Therefore, the method of counting the
169 rising edges of the 400 Hz signal directly to 400 ensures the precise generation of these rising edges.
170



171

172

173

174

4 Analysis of clock synchronization deviation

175

176

177

178

179

180

181

182

183

Fig.7 The schematic diagram of 1Hz synchronized signal generation.



184 processing, cable transmission and other stages that may generate signal delay, and it can be calculated
185 by the following equation:

$$186 \quad T = T_1 + T_2 + T_3 \quad (1)$$

187 where T is the delay of the generated 1 Hz square wave signal relative to the PPS, T_1 is the delay
188 generated by the circuit processing stage, T_2 is the delay generated by cable transmission, T_3 is the
189 delay caused by the signal passing through the transformers. T_1 mainly consists of three parts: chip
190 program processing, signal transmission in the circuit, power output synchronization signal process. T_1
191 can be calculated by the following equation:

$$192 \quad T_1 = T_c \times n + t_1 + t_2 \quad (2)$$

193 where T_c is the instruction cycle of the chip, i.e., the time required to execute one instruction, and n
194 is the number of instructions, t_1 is the delay caused by signal transmission in the circuit, t_2 is the delay
195 generated by high-power supply synchronization output. T_c is related to the crystal oscillator used by
196 the chip. In this paper, the value of T_c is 6 ns, the value of n doesn't exceed 30. t_1 is related to the
197 components used in the signal transmission path in the circuit board. In this paper, the value of t_1 doesn't
198 exceed 4 ns. There is a slight delay in the zero phase of the power supply output 400 Hz signal relative
199 to the rising edges of the 400 Hz synchronization signal, but the power supply output signal waveform
200 is not a standard sine wave, making it difficult to precisely identify the zero phase. Therefore, it is difficult
201 to obtain an accurate result for t_2 through separate test, but subsequent overall deviation test includes
202 t_2 . T_2 mainly consists of three parts: the delay caused by coaxial cable transmission, and delay caused
203 by wires transmission between circuit boards, and it can be calculated by the following equation:

$$204 \quad T_2 = \frac{L_{cable}}{v_{cable}} + \frac{L_{wire}}{v_{wire}} \quad (3)$$

$$205 \quad v_{cable} = \eta_1 \times c \quad (4)$$

$$206 \quad v_{wire} = \eta_2 \times c \quad (5)$$

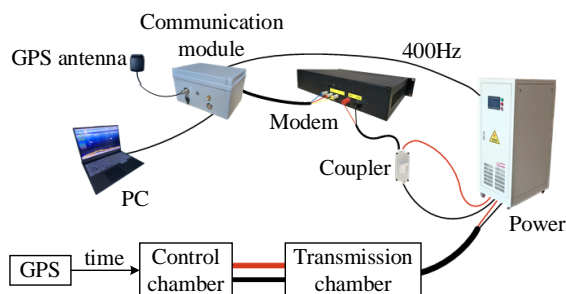
207 where L_{cable} is the length of coaxial cable, and v_{cable} is the speed at which the signal is transmitted
208 through the coaxial cable L_{wire} is the length of coaxial cable, and v_{wire} is the speed at which the signal
209 is transmitted via the coaxial cable, c is the speed of light in a vacuum, η_1 is the ratio of the speed of
210 signal transmission on coaxial cables to the speed of light in a vacuum, η_2 is the ratio of the speed of
211 signal transmission between circuit boards via wires to the speed of light in a vacuum. The typical value
212 of η_1 ranges from 0.67 to 0.75, and the typical value of η_2 ranges from 0.6 to 0.9 (when using 22AWG
213 wire). Therefore, for every 1 km of coaxial cable, the resulting delay typically falls within the range of
214 4.48 to 4.98 μ s. The total length of wires between circuit boards inside the transmission chamber doesn't
215 exceed 1 m, resulting in a delay typically range from 3.7 to 5.56 ns.

216 The 400 Hz signal output from the high-power supply passes through two stages of transformers and is
217 reduced to low voltage ranging from 0 to 22V for processing by the underwater signal processing unit.
218 The transformers are not ideal transformers, so there is a certain phase shift between the primary input
219 voltage and the secondary output voltage of each transformer, which is the cause of T_3 . Due to limited
220 test condition, T_3 can't be tested separately in this paper, but the subsequent overall deviation testing
221 includes T_3 . All deviations described above can be combined and measured in the overall test of the
222 clock synchronization method.

223 **5 The test of clock synchronization method**



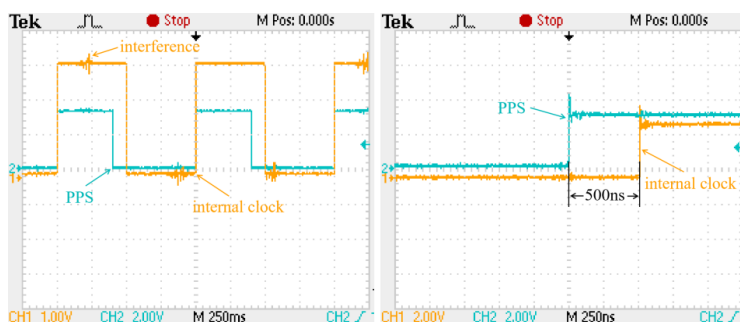
224 In accordance with the clock synchronization method using a power supply signal based on a coaxial
225 cable, as discussed in this paper, a test platform was built in the laboratory to evaluate the effectiveness
226 of clock synchronization. The test setup is shown in Fig.8. Due to the high voltage output of the power
227 supply and the low voltage requirement of the modem, a coupler is needed to connect the two (Giraneza
228 and Abo-Al-Ez, 2022; Costa et al., 2017). The coupler used is a capacitive coupler, which presents
229 significant impedance to the 400 Hz AC signal. Consequently, the voltage in the power carrier loop
230 primarily accumulates at the coupler's ends. Since the frequency of power line communication exceeds
231 100 kHz, the coupler's impedance is relatively low. Therefore, the power line communication signal can
232 pass through the coupler. The 400 Hz synchronization signal of the high-power supply does not pass
233 through the coupler, so the coupler does not cause a delay.



234
235
236

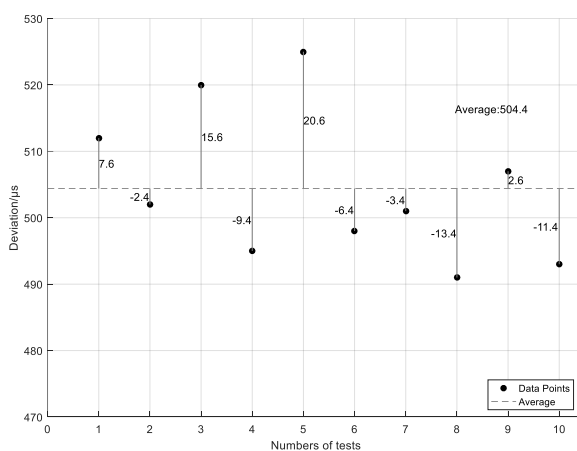
Fig.8 The diagram of test setup.

237 According to the predetermined operation process, the test system was powered on after the entire test
238 system was correctly connected. Once the control circuit received the 1 Hz PPS and recorded the specific
239 timing of the rising edges, the GPS module, which provided time to the control circuit, was removed,
240 and the high-power supply was activated. Fig.9 shows the internal clock synchronized with the PPS and
241 the clock synchronization deviation. To facilitate observation, the duty cycle of the internal clock signal
242 generated by the underwater signal processing unit was set to 50%, while the duty cycle of the PPS output
243 from the GPS module was set to 40%. After continuous observation, the deviation between the rising
244 edge of the internal clock signal and the rising edge of the PPS was approximately 504 ns. Fig.10 presents
245 the results of multiple tests, showing that that synchronization deviation fluctuated around 504 ns with a
246 range of 34 ns. The coaxial cable used in the test was relatively short. In marine operations, a 10 km
247 length of coaxial cable can introduce a maximum delay of approximately 49.8 μ s. In this case, the
248 maximum delay of internal clock signal relative to the PPS would be approximately 50.3 μ s. During the
249 measurement of the internal clock signal, some interference pulses were observed, likely caused by test
250 pins being too close to the high power equipment in the laboratory environment. Fig.11 includes some
251 photos from the test scene.
252 Unlike Scripps transmitter, this study employs a ship-borne high-power supply to transmit a 400 Hz
253 signal and generate a 1 Hz square wave synchronized with the PPS as the synchronization signal for the
254 transmitter circuit. The transmission waveform frequency control signal is generated based on the
255 internal crystal oscillator of the circuit, with its rising edge aligned with the rising edge of the 1 Hz
256 synchronization signal.



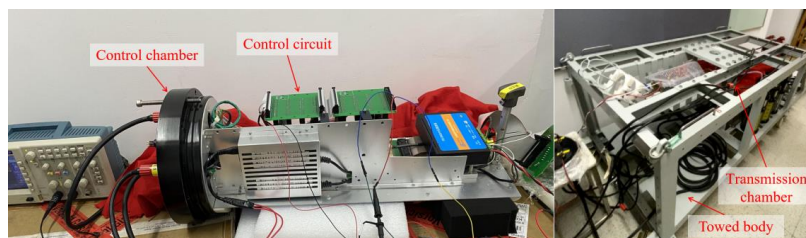
257
258
259

Fig.9 Internal clock synchronized with PPS (left); clock synchronization deviation (right).



260
261
262
263

Fig.10 The graph of multiple tests results for synchronization deviation, shows the difference between each result and the average value.



264
265
266

Fig.11 Control chamber (left); transmission chamber (right).

267 6 Conclusion

268 This paper introduces a clock synchronization method of marine controlled source electromagnetic
269 transmitter base on coaxial cable and build the hardware system. In this method, the ship-borne high
270 power-supply outputs the 400 Hz signal synchronized with PPS, and transmits it to the underwater
271 transmitter. The transmitter control circuit can generates a 1 Hz square wave signal synchronized with



272 PPS for clock synchronization. The delay deviation of the rising edges of the 1 Hz square wave signal
273 obtained by this method relative to the rising edges of PPS is less than 1 ms, which meets the requirement
274 for clock synchronization accuracy of better than 1ms in practical operations and can be used for internal
275 clock synchronization of the transmitter. This method has a positive effect on the future operation of
276 marine controlled source electromagnetic transmitters carrying more ships.

277 **7 Statement**

278 This manuscript satisfies the following statements that: 1) all authors agree with the submission, 2) the work
279 has not been published elsewhere, either completely, in part, or in another form, and 3) the manuscript has
280 not been submitted to another journal.

281 **Data availability**

282 No data sets were used in this article.

283 **Author contributions**

284 M. Wang is the project applicant and a key participant in the testing process. K. Chen provided some
285 optimization suggestions for the test scheme. C.T. Wang and R.Y. Yu, as the research assistants, had
286 helped complete the testing. Z.B. Ren is the project leader, primarily responsible for the test scheme
287 design, hardware circuit design, and other related tasks.

288 **Competing interests**

289 The contact author has declared that none of the authors has any competing interests.

290 **Financial support**

291 This work was supported by the National Natural Science Foundation of China (42374221), the Key
292 Technologies R&D Program (2022YFC2807900), Marine Economic Development in Guangdong
293 Province (Grant Number: GDNRC[2023]40).

294 **Acknowledgement**

295 Thanks to the editors and reviewers. Additionally, this paper was supported by south China sea institute
296 of oceanology, cas and Fujian earthquake agency. The authors express thanks to the two mentioned
297 institutions.

298 **References**

- 299 Amuta, E., Awelewa, A., Olajube, A., Somefun, T., Afolabi, G., and Uyi, A.: Power line carrier
300 technologies: a review, IOP Conference Series: Materials Science and Engineering, Ota, Nigeria, 27th-
301 28th July 2020, 012062, doi: 10.1088/1757-899X/1036/1/012062, 2021.
- 302 Chen, K., Deng, M., Wu, Z., Jing, J., Luo, X., and Wang, M.: Low Time Drift Technology for Marine
303 CSEM Recorder, *Geoscience*, 26, 1312-1316, doi: 10.3969/j.issn.1000-8527.2012.06.027, 2012.
- 304 Chen, K., Deng, M., Yu, P., Yang, Q., Luo, X. H., and Yi, X. P.: A near-seafloor-towed CSEM receiver
305 for deeper target prospecting, *Terrestrial Atmospheric and Oceanic Sciences*, 31, 565-577, doi:
306 10.3319/tao.2020.08.03.01, 2020.
- 307 Constable, S.: Marine electromagnetic methods—A new tool for offshore exploration, *The Leading Edge*,
308 25, 438-444, doi: 10.1190/1.2193225, 2006.
- 309 Constable, S.: Ten years of marine CSEM for hydrocarbon exploration, *Geophysics*, 75, 75A67-75A81,
310 doi: 10.1190/1.3483451, 2010.
- 311 Constable, S.: Review paper: Instrumentation for marine magnetotelluric and controlled source
312 electromagnetic sounding, *Geophysical Prospecting*, 61, 505-532, doi: 10.1111/j.1365-
313 2478.2012.01117.x, 2013.
- 314 Constable, S. and Srnka, L. J.: An introduction to marine controlled-source electromagnetic methods for
315 hydrocarbon exploration, *Geophysics*, 72, WA3-WA12, doi: 10.1190/1.2432483, 2007.



- 316 Costa, L. G. d. S., Queiroz, A. C. M. d., Adebisi, B., Costa, V. L. R. d., and Ribeiro, M. V.: Coupling for
317 power line communications: A survey, *Journal of Communication and Information Systems*, 32, doi:
318 10.14209/jcis.2017.2, 2017.
- 319 Cox, C., Constable, S., Chave, A., and Webb, S.: Controlled-source electromagnetic sounding of the
320 oceanic lithosphere, *Nature*, 320, 52-54, doi: 10.1038/320052a0, 1986.
- 321 Edwards, R. and Chave, A.: A transient electric dipole-dipole method for mapping the conductivity of
322 the sea floor, *Geophysics*, 51, 984-987, doi: 10.1190/1.1442156, 1986.
- 323 Ferreira, H. C., Grové, H. M., Hooijen, O., and Vinck, A. H.: Power line communication, Wiley
324 Encyclopedia of Electrical and Electronics Engineering, 16, 706-716, doi: 10.1002/047134608X.W2004,
325 2001.
- 326 Giraneza, M. and Abo-Al-Ez, K.: Power line communication: A review on couplers and channel
327 characterization, *AIMS Electronics and Electrical Engineering*, 6, 265-284, doi:
328 10.3934/electreng.2022016, 2022.
- 329 Kaddoum, G. and Tadayon, N.: Differential chaos shift keying: A robust modulation scheme for power-
330 line communications, *IEEE Transactions on Circuits and Systems II: Express Briefs*, 64, 31-35, doi:
331 10.1109/TCSII.2016.2546901, 2016.
- 332 Liu, Y.-H., Yin, C.-C., Weng, A.-H., and Jia, D.-Y.: Attitude effect for marine CSEM system, *Chinese*
333 *Journal of Geophysics*, 55, 2757-2768, doi: 10.6038/j.issn.0001-5733.2012.08.027, 2012.
- 334 Meng, W., Ming, D., Qi-sheng, Z., Kai, C., and Jin-ling, C. U. I.: The technique of time synchronization
335 operation to control marine electromagnetic emission, *Progress in Geophysics*, 24, 1493-1498, doi:
336 10.3969/j.issn.1004-2903.2009.04.043, 2009.
- 337 Meng, W., Ming, D., Qingxian, Z., Xianhu, L., and Jianen, J.: Two types of marine controlled source
338 electromagnetic transmitters, *Geophysical Prospecting*, 63, 1403-1419, doi: 10.1111/1365-2478.12329,
339 2015.
- 340 Qiu, Y., Yang, Q., Deng, M., and Chen, K.: Time synchronization and data transfer method for towed
341 electromagnetic receiver, *Review of Scientific Instruments*, 91, doi: 10.1063/5.0012218, 2020.
- 342 WANG, M., DENG, M., WU, Z.-L., LUO, X.-H., JING, J.-E., and CHEN, K.: New type deployed marine
343 controlled source electromagnetic transmitter system and its experiment application, *Chinese Journal of*
344 *Geophysics*, 60, 4253-4261, doi: 10.1111/1365-2478.12329, 2017a.
- 345 Wang, M., Deng, M., Wu, Z., Luo, X., Jing, J., and Chen, K.: The deep-tow marine controlled-source
346 electromagnetic transmitter system for gas hydrate exploration, *Journal of Applied Geophysics*, 137, 138-
347 144, doi: 10.1016/j.jappgeo.2016.12.019, 2017b.
- 348 WANG, M., WU, Z.-L., DENG, M., MA, C.-w., LIU, Y., and WANG, S.-x.: The high precision time stamp
349 technology in MCSEM transmission current waveform, *Progress in Geophysics*, 30, 1912-1917, doi:
350 10.6038/pg20150452, 2015.
- 351 Wang, M., Zhang, H.-Q., Wu, Z.-L., Sheng, Y., Luo, X.-H., Jing, J.-E., and Chen, K.: Marine controlled
352 source electromagnetic launch system for natural gas hydrate resource exploration, *Chinese Journal of*
353 *Geophysics*, 56, 3708-3717, doi: 10.6038/cjg20131112, 2013.
- 354 Wang, M., Ming, D., Li, X., Zhang, Z., Yue, H., Zhang, T., Duan, N., and Ma, X.: The latest development
355 of Marine controllable source electromagnetic transmitter, *IOP Conference Series: Earth and*
356 *Environmental Science*, Changchun, China, 11-14 October 2020, 012137, doi: 10.1088/1755-
357 1315/660/1/012137, 2021.

358